Astron. Astrophys. 351, 627–634 (1999)

ASTRONOMY AND ASTROPHYSICS

Irregular variables of type Lb

Energy distributions and stellar parameters

F. Kerschbaum

Institut für Astronomie der Universität Wien, Türkenschanzstrasse 17, 1180 Wien, Austria

Received 18 August 1999 / Accepted 28 September 1999

Abstract. AGB variables of types Lb, SRa, SRb, and Mira are studied by fitting combinations of blackbodies to visual, near infrared and IRAS data. This paper supplements an earlier work dealing with a smaller sample of SRa and SRb variables. The fitted parameters T^*, $T^{\rm d}$ and R^d/R^* are related to physically meaningful quantities. Also, quantities derived from the fits like the ratio of the luminosities of the two fitted blackbodies are confronted with independent mass-loss estimators.

For the O-rich Lb variables all of the 'blue' objects can be reasonably well approximated by only one blackbody whereas the 'red' ones need two. Among the 'blue' objects a significant fraction seem to be not on the AGB at all but a kind of 'RGB pollution'. The T^* values, reflecting mainly offseted (-500 K) effective temperatures for objects with small to moderate mass-loss, are significantly higher in the 'blue' cases.

Carbon-rich objects differ significantly from the O-rich ones in their fit parameters. Sometimes 'unphysically' low T^* are found – a result of circumstellar reddening in the high mass-loss cases. Furthermore lower values of $T^{\rm d}$, accompanied by normal T^*s and large shell radii are common and can be related to the phenomenon of detached shells. S-stars populate a similar region to the optically thin carbon stars in their fit properties.

Key words: stars: AGB and post-AGB – stars: variables: general – stars: mass-loss – infrared: stars

1. Introduction

The Semiregular variables of types SRa and SRb (SRV) and the Irregular variables of type Lb (IRV) are quite numerous groups of objects among the stars on the AGB. They can provide important constraints for theoretical mass-loss models due to their different pulsational behaviour compared to the more frequently studied Mira variables. In a series of papers (Kerschbaum & Hron 1992, 1994, 1996, hereafter SR_I, SR_IIa, and SR_III, respectively; Kerschbaum 1995, hereafter SR_IIb) the SRVs have been studied in a broad and systematic way. This made it possible to divide this inhomogeneous group of objects into physically distinct classes, based on stellar properties and galactic distribution. For the O-rich stars the subclasses 'blue'-, 'red'-, and 'Mira'-SRVs were introduced. The 'blue' subclass contains objects with short periods (typically below 100^d) and no apparent signs of mass-loss. The border between 'red'- and 'Mira'-SRVs is mainly defined by the period (P$<200^d$ for 'red', and P$>200^d$ for 'Mira'). The 'blue'-SRVs seem to be on the early AGB, while the other two groups are probably on the thermally pulsing AGB. Jura & Kleinmann (1992) reached the same conclusions concerning the galactic distribution of these stars.

Work on the IRVs is complicated by the larger contamination by poorly observed late-type variables [to some extent this applies also to the SRVs, Lebzelter et al. (1995)]. Kerschbaum et al. (1996b, hereafter Lb_I) found that their sample of visually bright IRVs displays infrared properties very similar to the SRVs. There may be a slightly larger 'contamination' with non-AGB giants than in the case of the SRVs, but the AGB objects seem to resemble the 'blue' and the 'red' SRVs. In a conference contribution by Kerschbaum et al. (1996a) – based on NIR- and IRAS-photometry – full spectral energy distributions, mass-loss rates, and galactic distributions were analyzed, and the similarity between the IRVs and SRVs was further demonstrated.

The gas mass-loss properties of both the semiregular and irregular variables where investigated in detail during the last years. E.g. Kerschbaum et al. (1996c, hereafter SR_IV) surveyed the circumstellar CO emission of O-rich SRVs. The majority of their detected objects, covering both small and longer periods, are low mass-loss rate objects ($\lesssim 10^{-7}\,{\rm M}_\odot\,{\rm yr}^{-1}$), and low expansion velocity envelopes (the mean value is $\sim$8 km s^{-1}). A significant number of C-rich SRVs and IRVs was included in the survey of Olofsson et al. (1993). O-rich IRVs were for the first time studied in circumstellar CO by Kerschbaum & Olofsson (1998). They found that their mass-loss properties are very similar to those of O-rich SRVs and (optically bright) Miras, i.e., at least in this mass-loss rate range the stellar mass-loss properties are not strongly influenced by the pulsational behaviour of the star. In Kerschbaum & Olofsson (1999) a catalogue of circumstellar CO observations of SRVs and IRVs was presented including brief discussions on detection statistics, line profiles, gas expansion velocity distributions, and correlations between CO line and IR continuum fluxes.

Send offprint requests to: kerschbaum@astro.univie.ac.at

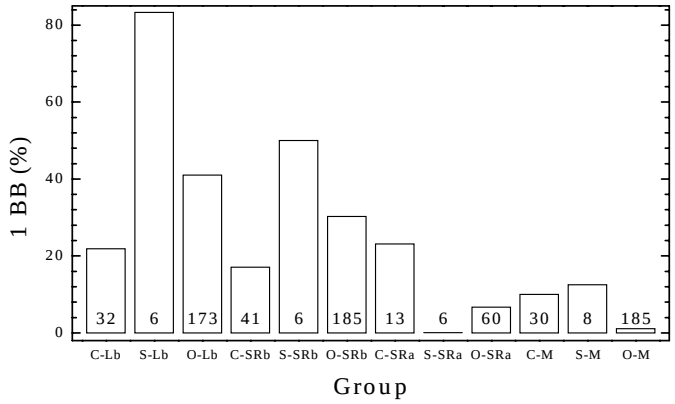

Fig. 1. Percentage of fits with one blackbody for the main chemistry groups of the Lb, SRa, SRb and Mira variables. The number in the bin gives the total number of objects for the given group.

2. Blackbody fits

As already done for the SRVs in SR_II a fit of combinations of two blackbodies to the spectral energy distribution (SED) defined by visual and infrared data can lead to a simple description of the IRVs in terms of astrophysical quantities like effective temperature or dust mass-loss rate. An earlier application of BB-fits to AGB-star SEDs is found e.g. in Epchtein et al. (1987).

2.1. The data

Three main data sources are used within this paper. The visual information (mostly V, B or P ($m_{\rm pg}$)) is taken from the GCVS4, near infrared JHKL′(M)-photometry comes mainly from papers Lb_I, SR_IIa, and SR_IIb. These data sets are supplemented by newer own unpublished material on SRVs and IRVs as well as data on Miras from Fouqué et al. (1992) and Guglielmo et al. (1993). Finally, mid and far infrared measurements were extracted from the IRAS-PSC (1988). The values for the absolute calibration were taken from Lamla (1982), Le Bertre (1988) and the IRAS-EXP (1988) for the visual, the NIR and the IRAS-range, respectively.

2.2. The method

For a more detailed introduction see SR_II. Here we give only a short summary.

The overall spectra can be roughly fitted by a 'photospheric' temperature T^*, a 'dust'-temperature $T^{\rm d}$ and the 'size' of the circumstellar shell relative to the star $r = R^d/R^*$:

$$\nu F_\nu = const \cdot \frac{1}{\lambda^4} \cdot \left(\frac{1}{e^{hc/\lambda k T^*} - 1} + \frac{r^2}{e^{hc/\lambda k T^d} - 1} \right), \quad (1)$$

where F is the monochromatic flux, λ the wavelength and ν the frequency. c, h and k stand for the speed of light, the Planck and the Boltzmann constant, respectively. The quantity $\nu F_\nu = \lambda F_\lambda$ is independent of the units of wavelength or frequency and gives the energy emitted in equal logarithmic intervals of ν or λ. As one can see later in the plots of real energy distributions (Fig. 7), it is useful for spectra extending over a large wavelength range.

The automatic nonlinear least square fits of these two blackbodies can also lead to a fit with only one blackbody if a fit with two blackbodies does not seem significant (see again SR_II). The filter M was omitted for the fits because in most of the cases it was not possible to reproduce the M measurements – usually on the low side – with our fits of two blackbodies. The CO fundamental vibrational-rotational band in the region around 4.6 μm (e.g. Cohen et al. 1992) is probably responsible for this general trend.

The results of the individual fits are available in electronic form from the author upon request. The ascii-table contains object name, $const$, T^*, $T^{\rm d}$, r, and $L^{\rm d}/L^*$ (see below).

2.3. Physical interpretation of the fit-parameters

The resulting parameters T^*, $T^{\rm d}$ and r of course need to be related to astrophysically meaningful quantities. As shown in SR_II for O-rich SRVs, our 'photospheric' temperature T^* can be corrected to an estimate of the effective temperature by adding about 500 K.

A similar comparison was made for the C-rich objects. Here the resulting offset is of the same order and direction as in the case of O-rich stars, namely about 460 K. In all the following plots and also in the discussion one has to keep in mind these corrections if one is interested in real effective temperatures!

For the parameters related to the circumstellar material, namely the 'dust'-temperature $T^{\rm d}$ and the 'size' of the circumstellar shell relative to the star $r = R^d/R^*$, the situation is more complex. In SR_II a comparison of BB-fits with the results of dust shell models indicated that both correspond to a region in the innermost part of the dust shell. It should be noted however, that these results are preliminary.

Another useful byproduct of blackbody-fits is the apparent bolometric magnitude of the objects which can be used to derive bolometric luminosities when the distances are known (e.g. Kerschbaum et al. 1997).

2.4. Overall properties of the fits

In Fig. 1 the percentage of fits with one blackbody for the main chemistry groups of IRVs, SRVs and Miras is presented. The number in the bin gives the total number of objects for the given group.

Significant differences are obvious. In the O-rich cases, Lb and SRb variables contain a large fraction of objects best fitted by only one blackbody (1 BB) whereas the SRa's and even more the Miras mostly need two blackbodies. The dustless 1BB objects are similar to the 'blue' SRVs defined in our earlier papers.

Fig. 2 shows the detailed distribution of the resulting fit parameters for all our stars having near infrared photometry. Again individual results are plotted for the main chemistry groups. If one wants to compare the plotted T^* temperatures with real ef-

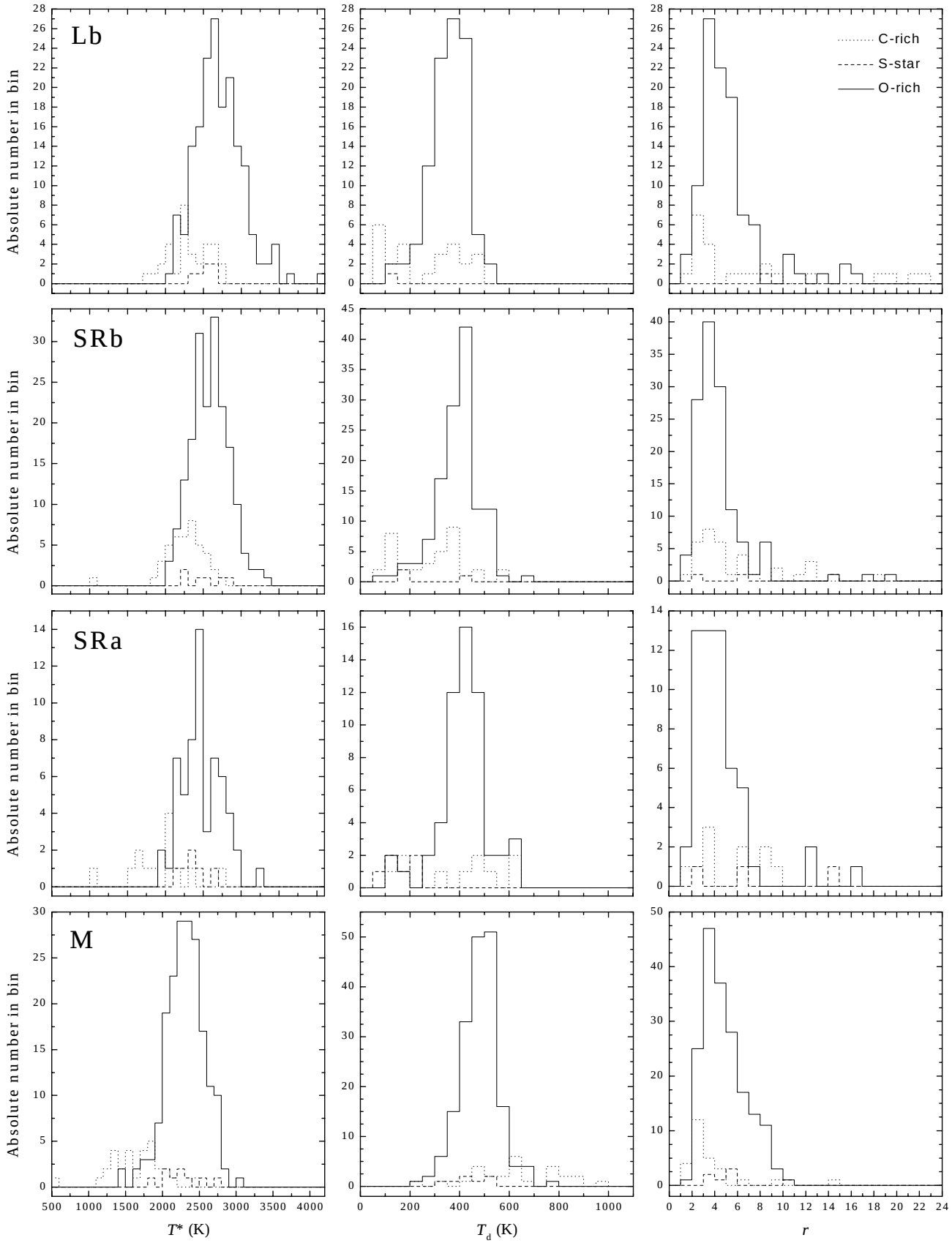

Fig. 2. Distribution of the three blackbody fit parameters: 'photospheric' temperature T^*, 'dust'-temperature $T^{\rm d}$ and relative 'size' of the dust shell $r = R^d/R^*$. Three different linestyles denote C-rich and S-, O-rich stars respectively.

fective temperatures one has to apply the corrections given in the previous section.

The most remarkable result is the large fraction of O-rich Lb and to a lesser extent SRb stars exhibiting high T^* values. The most extreme cases may not be on the AGB at all (compare Lb_I). As mentioned above most of these dustless objects can be described by one blackbody. A temperature T^* of about 2500 K marks the cool temperature end of the 'blue' O-rich SRVs – hence nearly half of the observed O-rich IRVs seem to have similar 'blue' properties. The rest of the O-rich IRVs shows T^* values comparable to the 'red' SRVs. Generally we see a falling sequence in T^* when going from Lbs to SRbs, to SRas and finally to the Miras. Among the last group a large fraction can be fitted with unphysically low T^* values – probably a result of circumstellar extinction around these (on the average) higher mass-loss rate objects. The $T^{\rm d}$ values show more or less the opposite trend – the lowest mean is found for the Lbs. For O-rich objects the r values differ not significantly.

In all variability groups the carbon stars have been fitted with significantly lower T^*. This result can be explained by the cooler temperature of carbon star atmospheres. Especially the C-SRas and C-Miras can be fitted only with unphysically low T^* – probably again a result of circumstellar extinction around these high mass-loss objects.

The $T^{\rm d}$ distributions for all C-rich objects but the Miras extend towards very low values. In these cases the r values show an anti-correlated behaviour (i.e. low $T^{\rm d}$ coincides with high r). In the Lb and the SRb r-plot two objects VY UMa and TT Cyg are missing because of their extreme r-values of 40 and 64, respectively. It turns out that r-values over 15 and $T^{\rm d}$ values below 150 K often indicate the presence of detached circumstellar shells around the C-rich objects [e.g. TT Cyg (Olofsson et al. 1990)]. A few comments on such objects are found below (see also Fig. 7 for the SED of VY UMa).

The distribution of the fit parameters of the S-type stars is similar to that of the C-rich stars with a tendency to cooler $T^{\rm d}$ values, although the small number of objects does not allow any definite statements.

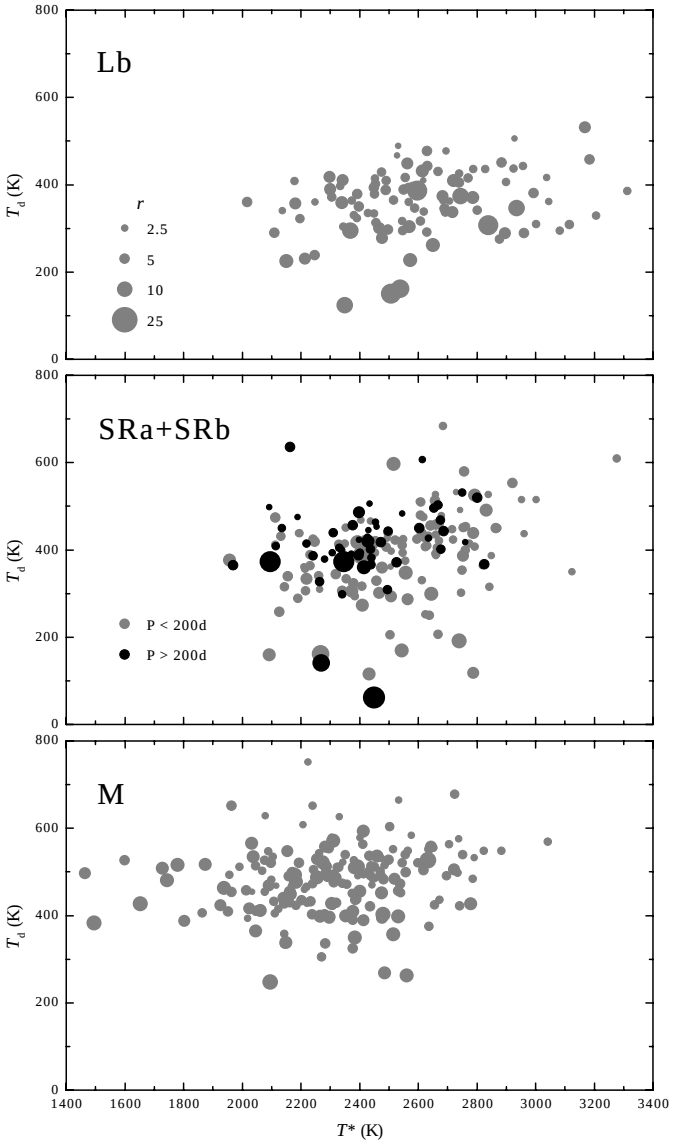

Fig. 3. 'Dust'-temperature $T^{\rm d}$ as a function of 'photospheric' temperature T^* with the relative 'size' of the dust shell R^d/R^* indicated by the size of the plot symbols for the three O-rich groups of variables.

2.5. Oxygen-rich stars

For the O-rich variability groups (SRa+SRbs combined and split in two period groups) the 'dust'-temperature is plotted versus the 'photospheric' temperature in Fig. 3. The 1BB-fits are not shown in these diagrams for obvious reasons. The area of the circles is linearly proportional to the relative 'size' r of the dust shell with respect to the photosphere. Keeping in mind the limitations of that very simple approach some characteristics can be deduced.

First of all, for 41 % of the IRVs the automatic fit procedure leads to fits with only *one*, relatively 'hot' blackbody – the remaining 59 % have a distribution similar to that of the short period SRVs but extending towards higher T^*. Extreme 1BB-cases may not even be AGB stars – μ Mus ($T^* = 3620$ K) is shown in Fig 7. This object has only 490 $L_\odot$ when combining its Hipparcos parallax of 7.55 mas with its apparent bolometric magnitude of -2.0 mag derived by integrating its SED from the visual to the far infrared! Its maybe the prototype of the 'RGB pollution' among the Lb variables.

As for the SRVs also in the O-rich IRV sample a few objects have quite low $T^{\rm d}$ values, namely BC And ($T^* = 2510$ K, $T^{\rm d} = 150$ K, $r = 15$), V590 Cyg (2350, 120, 10), V1172 Cyg (2540, 160, 14), and BB Dra (2500, 150, 6). The IRAS photometry of V1172 Cyg may be influenced by galactic cirrus which could also cause its 60 and 100 μm excess. The others should be checked for cold extended circumstellar material (see below).

With a few (1 %) exceptions, not plotted here, only fits with *two* blackbodies are found for Miras. Their colder T^* values are due to both true lower effective temperatures and, below about 2200 K, to reddening by circumstellar material which mimics

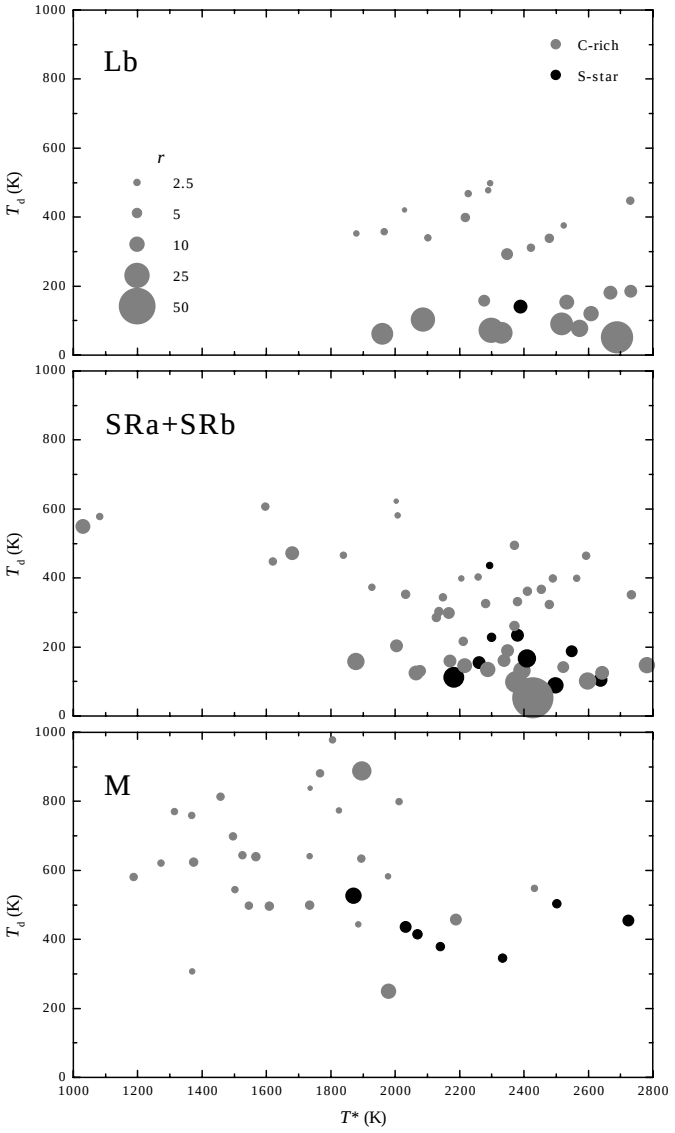

Fig. 4. 'Dust'-temperature $T^{\rm d}$ as a function of 'photospheric' temperature T^* with the relative size of the dust shell R^d/R^* indicated by the size of the plot symbols for C-rich objects (shaded in gray) and S-stars (black).

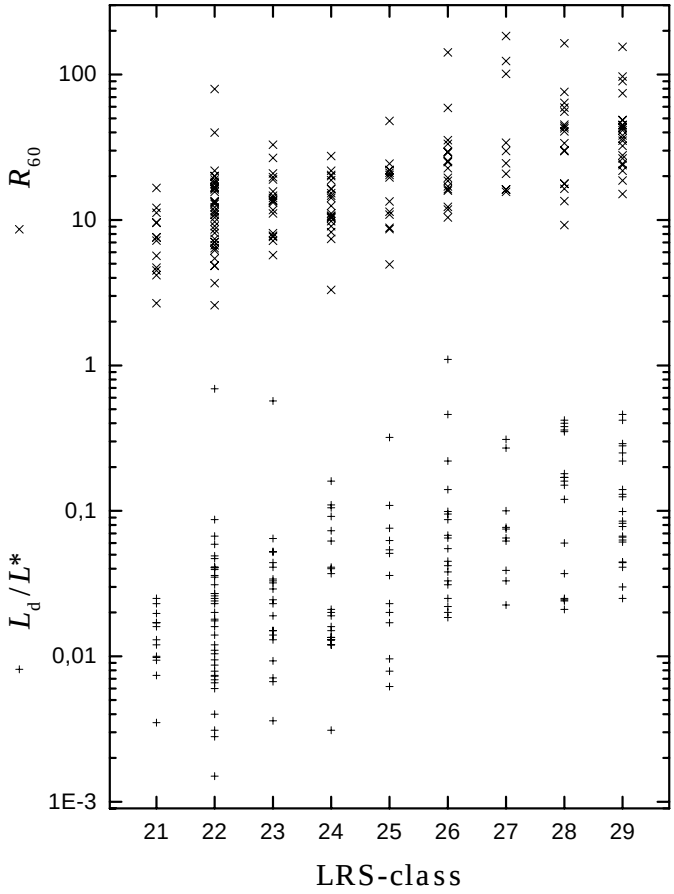

Fig. 5. Correlation of the IRAS LRS-class and the ratio of the luminosities $L^{\rm d}/L^*$ of the fitted blackbodies and the flux ratio at 60 μm, R_{60}, for O-rich objects.

these unphysically low, fitted temperatures. The higher $T^{\rm d}$ values for low T^* have the same reason – high mass-loss.

2.6. S-stars and carbon-rich stars

The situation of the carbon and S-stars is quite different from that of the O-rich ones. Fig. 4 displays the distribution of the fit parameters for C- and S-stars with the latter shaded in black.

Only the carbon stars fitted with *two* blackbodies are shown (about 80 % on average). Two main regions are obvious: first, that of objects with weak circumstellar emission at $T^* > 2000$ K. These stars have optically thin envelopes with increasing R^d/R^* for lower $T^{\rm d}$. This result is not an artefact of the fit procedure but represents significant physical differences. The most extreme example is the carbon SRb variable TT Cyg (2380, 50, 64; see also Fig. 10 in SR_III) with its detached circumstellar shell also observed in CO (Olofsson et al. 1990). Consequently, W Pic (1960, 60, 19), DR Ser (2090, 100, 22), U Ant (2300, 70, 25), HK Lyr (2330, 65, 19), TV Lac (2520, 90, 22), and VY UMa (2690, 50, 40) among the C-rich IRVs would be candidates for this phenomenon.

The far infrared IRAS fluxes of DR Ser and HK Lyr may suffer from weak galactic cirrus. U Ant is a well known C-star with detached circumstellar material (e.g. Olofsson et al. 1990, Izumiura et al. 1997). W Pic is one of the objects resolved in the IRAS survey data (Young et al. 1993).

The left part of the Fig. 4, at T^* below 2000 K, is the region of objects suffering heavy mass-loss. Reddening by the circumstellar material is responsible for their physically meaningless low T^* (compare with Knapik et al. 1999). No Lbs and only a few SRVs are found in this region which is mainly a IR-Mira domain.

For S-stars we are dealing with small numbers, nevertheless a few trends are clear. S-Lbs are mostly (80 %) fitted by only 1 BB, also S-SRbs have a high 1 BB percentage (50 %). The SRas and Miras are again dominated by higher mass-loss objects. They mostly populate the same area as the carbon stars only avoiding the very high mass-loss area. This supports Jura's

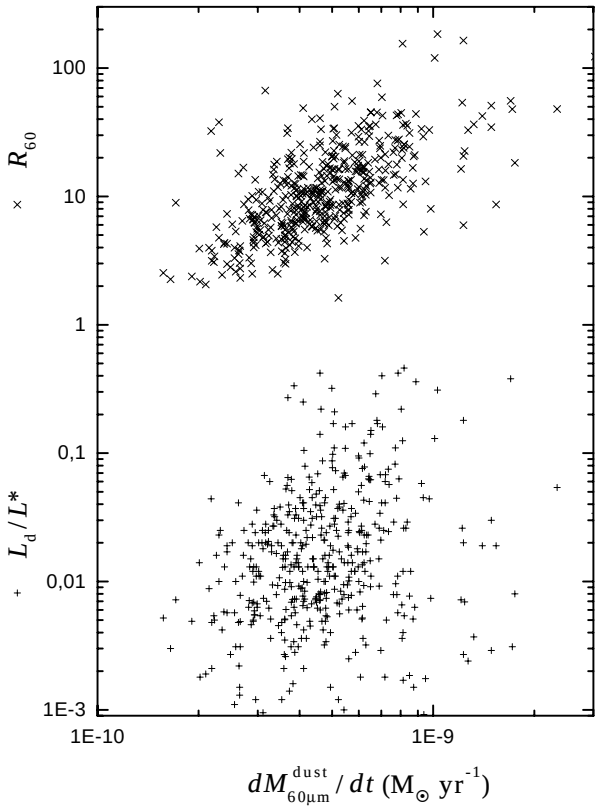

Fig. 6. Correlation of the dust mass-loss rate derived from the corrected IRAS F_{60} flux and the ratio of the luminosities $L^{\rm d}/L^*$ of the fitted blackbodies and the flux ratio at 60 μm, R_{60}, for O-rich objects.

(1988) results obtained from an IR-study of mass-loss from S stars. He came to the conclusion that the circumstellar dust around S stars is more nearly like that around C-rich red giants than that around O-rich ones. The distribution extends down to very low $T^{\rm d}$ values. CX Mon (2390, 140, 8) is the only S-Lb SED fitted with two BB.

2.7. Blackbody fits and mass-loss

An interesting result of the fit procedure is the ratio of the luminosities of the two fitted blackbodies $L^{\rm d}/L^*$. For low mass-loss objects it should be a good measure of the 'dustiness' and hence mass-loss rate of the objects. Another deducible quantity is the flux ratio of the stellar and the circumstellar contribution at 60 μm, $R_{60} = F^{\rm d}_{60}/F^{\star}_{60}$. It also should be a mass loss indicator in the sense that for stars with small mass-loss rates, the stellar contribution to the flux at 60 μm should not be negligible. The latter ratio is also of high importance if one tries to derive mass-loss rates from the 60 μm flux using simple formulae which assume that all flux at 60 μm originates from the dust (compare e.g. SR_IV and Lb_II). For low mass-loss objects this assumption is not valid any longer and a correction should be applied.

One independent check for how well these two parameters are correlated with the mass-loss rate is a comparison with the strength of certain dust features (e.g. silicate or SiC emission) used for the IRAS-LRS classification of types $2n$, $3n$ and $4n$. In Fig. 5 both quantities $L^{\rm d}/L^*$ and R_{60} are plotted for all our O-rich variables which are classified as $2n$ (optically thin silicate emission) in IRAS-LRS.

In the well populated O-rich $2n$-class the $L^{\rm d}/L^*$ ratio as well as the flux ratio R_{60} increase with the feature strength n. The contribution of the 'dust' blackbody to the total luminosity grows from 1 % to 10 % when going from LRS 21 to 29 class!

R_{60} varies from 7 to about 50 in the range of the $2n$ LRS classes. A good correlation is again obvious. Especially in the low mass-loss domain (left part of diagram) the correction of the IRAS F_{60} flux by subtracting the stellar contribution (up to 15 % in the low $2n$) is important – especially if one wants to derive mass-loss rates out of the IRAS flux at 60 μm (e.g. Jura 1987). Although not shown in a figure the $1n$ objects indicate the need for even higher corrections (20 % and more).

When using such a formula to derive dust mass-loss rates (compare SR_IV, Lb_II) one can also compare the derived rates with the above mentioned fit quantities. This is now not fully independent as in the case of IRAS LRS-classes but is still a consistency check. The corresponding plots are shown in Fig. 6.

Again a relatively good correlation is found for R_{60} but the luminosity ratio $L^{\rm d}/L^*$ indicates only a not very strict upper envelope. The later is probably caused by 'wrong' stellar BB fits in the higher mass-loss cases. In such cases the stellar BB sometimes includes significant contributions from the dust because of extinction effects (see above). This then leads to an underestimate of the dust BB.

For the C-rich $4n$ stars the correlation is not of comparable quality but at least the tendency goes in the same direction.

Summarizing, the LRS-class and the mass-loss rates derived from IRAS 60 μm flux confirm that the quantities $L^{\rm d}/L^*$ and R_{60} are indeed measures of the mass-loss rate. This gives additional support for the physical relevance of the crude approximation of real stars with combinations of blackbodies.

2.8. Examples of spectral energy distributions

In Fig. 7 six examples of energy distributions of different types of IRVs are displayed. Our examples on the left hand side are O-rich stars, those on the right hand side C-rich ones.

μ Mus, one of these 'very blue' O-rich IRVs which are probably RGB and not AGB stars (see LB_I) has a small amplitude (0.2 mag in V), a visual spectral type as early as K4III and a featureless LRS type of 18 without any indication of mass-loss. This object has only 490 $L_\odot$ when combining its Hipparcos parallax of 7.55 mas with its apparent bolometric magnitude of -2.0 mag derived by integrating its SED from the visual to the far infrared!

RW Vir has spectral properties between that of 'blue' and 'red' O-rich SRVs, a visual type of M5III, noticeable 10 μm emission from an optically thin O-rich envelope. Its light amplitude is somewhat larger and amounts to 0.7 mag in V.

UV Car is an O-rich, 'red' IRV according to our SRV classification. Its spectral type (M3-M5) supports this, whereas its

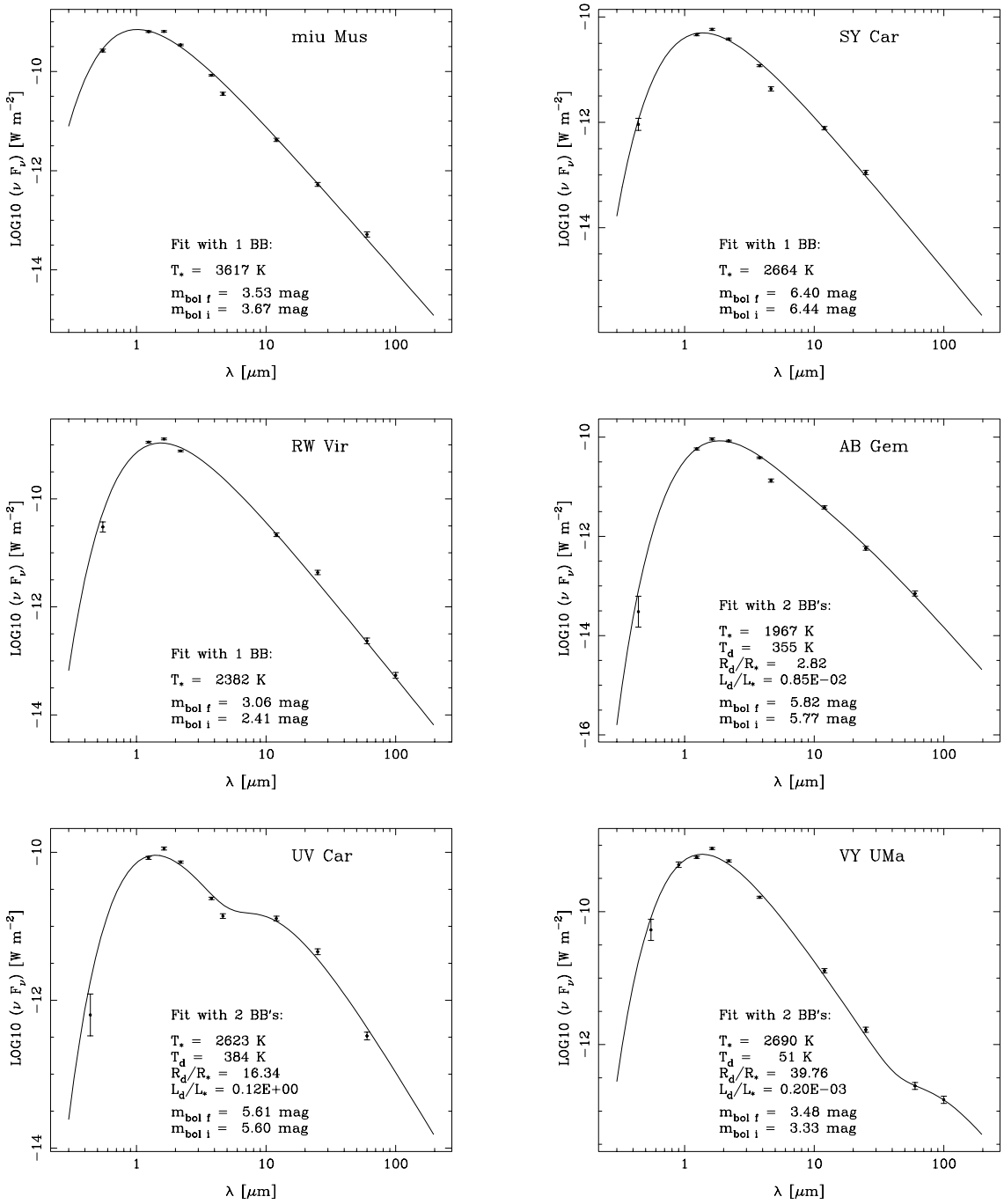

Fig. 7. Examples of some energy distributions of Irregulars, on the left hand side are O-rich stars, on the right hand side C-rich ones.

very strong 10 μm feature (LRS 29), and its large P-light amplitude of 2 mag places it even close to 'Mira-like' SRVs.

SY Car is a carbon Lb (C(N3)) with no indication of circumstellar material (from IRAS data). It has a small light amplitude of 0.8 mag in P.

AB Gem is a late type carbon Lb variable (C5,4(N3)) with strong circumstellar SiC feature (LRS 45). Its large P-amplitude of 2.2 mag is approaching Mira values. Its unphysically low $T^{\star}$ is caused by the circumstellar extinction of this high mass-loss object.

VY UMa's spectral energy distribution resembles that of SRVs with detached circumstellar CO-shells like the famous TT Cyg (Olofsson et al. 1990). This carbon Lb variable (C6,3(N0)/LRS 42) has a V-amplitude of 1.13 mag.

3. Conclusion

As already shown in SR_III, approximating the energy distributions of AGB-stars by two blackbodies is not only useful for predicting fluxes at wavelengths where no data are available.

Table 1. Typical fit properties of the larger groups.

Group	BB	n	T^* [K]	$T^{\rm d}$ [K]
'blue' IRV	1	52	2600–3150	
'red' IRV	2	92	2300–2800	300–450
'blue' SRV	1	50	2600–3000	
'red' SRV	2	121	2300–2750	300–500
'Mira' SRV	2	51	2250–2600	350–500
O-Mira	2	162	2050–2550	400–550
S-IRV	1	5	2500–2650	
S-SRV	2	9	2250–2550	100–300
S-Mira	2	7	1950–2550	350–500
C-IRV	2	25	2100–2600	100–400
C-SRV	2	44	1800–2550	150–450
C-Mira	2	27	1400–2000	450–800

At least for the objects studied so far this can also provide a reasonable description of the objects in terms of effective temperature, size and temperature of the dust shell and mass-loss rate. Thus blackbody fits can be considered as a preliminary stage to the much more elaborate technique of radiative transfer calculations.

The different energy distributions of the O-rich classes show up clearly in the blackbody fits. All 'blue' objects can be reasonably well approximated by only *one* blackbody whereas the 'red' and the 'Mira' like objects need *two*. Among the O-rich Lb variables a significant fraction seems to be RGB or early AGB objects without any indication of mass-loss and relatively high T^* values, reflecting mainly the offsetted (-500 K), effective temperatures. The rest of the O-rich Lbs populate the 'red' SRV domain and seem indistinguishable from them.

Carbon-rich objects differ significantly from the O-rich ones in their fit parameters. Especially for Miras sometimes 'unphysically' low T^* are found – a result of circumstellar reddening in the high mass-loss cases. Lower values of T^d, accompanied by normal T^* and large r are common among Lbs and SRVs – the most extreme examples being U Ant (Lb) and TT Cyg (SRb) with their detached envelopes. Finally, S-stars populate a similar region as the low and intermediate mass-loss carbon stars.

Table 1 summarizes the temperatures resulting from the fit procedures. The O-rich objects IRVs and SRVs were split in 'blue', 'red' and 'Mira' groups when possible. 'blue' stands for objects bluer than -1.2 in the IRAS [12]–[25] colour 'red' are those redder than -1.2 and having periods shorter than 200 days (no period in the case of the IRVs). 'Mira' SRVs are 'red' SRVs with longer periods (compare with SR_I).

For the future we plan on the one hand more detailed studies on interesting objects selected on the basis of their fit properties and on the other hand radiative transfer calculations of the envelopes of a subsample of IRVs and SRVs in order to probe for the physical properties of circumstellar dust. The observational material needed for the latter comes preferably from the ISO mission.

Acknowledgements. The author is grateful to the referee Dr. T. Lloyd Evans for valuable comments. This work was supported by APART (Austrian Programme for Advanced Research and Technology) from the Austrian Academy of Sciences, the Österreichische Nationalbank under the Jubiläumsfonds-project number 6876 and the Fonds zur Förderung der wissenschaftlichen Forschung under project number S7308-AST. We used the Simbad database operated at CDS, Strasbourg, France.

References

Cohen M., Witteborn F.C., Augason G., et al., 1992, AJ 104, 2045
Epchtein N., Le Bertre T., Lepine J.R.D., et al., 1987, A&AS 71, 39
Fouqué P., Le Bertre T., Epchtein N., Guglielmo F., Kerschbaum F., 1992, A&AS 93, 151
Guglielmo F., Epchtein N., Le Bertre T., et al., 1993, A&AS 99, 31
IRAS Science Team, 1988, IRAS Catalogs and Atlases, NASA RP–1190 (IRAS-PSC, IRAS-EXP)
Izumiura H., Waters L.B.F.M., de Jong T., Bontekoe Tj.R., Kester P., 1997, A&A 323, 449
Jura M., 1987, ApJ 313, 743
Jura M., 1988, ApJS 66, 33
Jura M., Kleinmann S.G., 1992, ApJS 79, 105
Kerschbaum F., Hron J., 1992, A&A 263, 97 (SR_I)
Kerschbaum F., Hron J., 1994, A&AS 106, 397 (SR_IIa)
Kerschbaum F., 1995, A&AS 113, 441 (SR_IIb)
Kerschbaum F., Hron J., 1996, A&A 308, 489 (SR_III)
Kerschbaum F., Habison P., Hron J., 1996a, Proc.: The Carbon Star Phenomenon. IAU Symposium 177, Kluwer Academic Publishers, Dordrecht, in press
Kerschbaum F., Lazaro C., Habison P., 1996b, A&AS 118, 397 (Lb_I)
Kerschbaum F., Olofsson H., Hron J., 1996c, A&A 311, 273 (SR_IV)
Kerschbaum F., Olofsson H., Hron J., 1997, In: Sasselov D.D., Takeuti M. (eds.) Proc. of of JD24, 23rd GA of the IAU, 17.–30.8.1997, Kyoto, Japan, Universal Academy Press Inc., Tokyo, Japan, p. 177
Kerschbaum F., Olofsson H., 1998, A&A 336, 654 (Lb_II)
Kerschbaum F., Olofsson H., 1999, A&AS 138, 299
Knapik A., Bergeat J., Butily B., 1999, A&A 344, 263
Lamla E., 1982, In: Schaifers S.K., Voigt H.H. (eds.) LB 2b, Springer, p. 73, Table 39, ref. k
Le Bertre T., 1988, A&A 190, 79
Lebzelter T., Kerschbaum F., Hron J., 1995, A&A 298, 159
Olofsson H., Carlström U., Eriksson K., Gustafsson B., Willson L.A., 1990, A&A 230, L13
Olofsson H., Eriksson K., Gustafsson B., Carlström U., 1993, ApJS 87, 267
Young K., Phillips T.G., Knapp G.R., 1993, ApJ 409, 725